Single-ion bound states in $S=1$ Heisenberg antiferromagnetic chains with planar anisotropy and subcritical exchange coupling

M. Orendáč
Department of Experimental Physics, P. J. Šafárik University, Park Angelinum 9, 041 54 Košice, Slovakia

S. Zvyagin
Institute for Low Temperature Physics and Engineering, Ukrainian Academy of Sciences, 47 Lenin Avenue, 310164 Kharkov, Ukraine and Physikalisches Institut der J. W. Goethe Universität, Robert-Mayer-Strasse 2-4, D-60054 Frankfurt am Main, Germany

A. Orendáčová
Department of Experimental Physics, P. J. Šafárik University, Park Angelinum 9, 041 54 Košice, Slovakia

M. Sieling and B. Lüthi
Physikalisches Institut der J. W. Goethe Universität, Robert-Mayer-Strasse 2-4, D-60054 Frankfurt am Main, Germany

A. Feher
Department of Experimental Physics, P. J. Šafárik University, Park Angelinum 9, 041 54 Košice, Slovakia

M. W. Meisel
Department of Physics and Center for Ultralow Temperature Research, University of Florida, P.O. Box 118440, Gainesville, Florida 32611-8440

(Received 23 November 1998)

Electron-spin-resonance (ESR) and magnetic-susceptibility data of single crystal of $Ni(C_2H_8N_2)_2Ni(CN)_4$, an $S=1$ Heisenberg chain system with strong planar anisotropy D, are presented. For sufficiently low magnetic field, the ESR spectrum is dominated by (anti)excitons as the elementary excitations from the singlet ground state. When the field exceeds a certain critical value $B_c \approx 4.5$ T, the ground state changes into a fully saturated ferromagnet, and magnons become the elementary excitations. An anomalous resonance line, observed for $B>4$ T, is identified as the transition between one-magnon and single-ion bound states. Good agreement exists between the ESR data and the corresponding theoretical predictions using the D and the nearest-neighbor exchange J values obtained by the analysis of existing thermodynamic data. In addition, the potential influence of in-plane anisotropy is discussed. The results are interpreted as experimental evidence of single-ion bound states in an $S=1$ planar Heisenberg chain with subcritical exchange coupling.
[S0163-1829(99)00830-9]

I. INTRODUCTION

The static and dynamic properties of one-dimensional magnetic systems have been the subject of theoretical and experimental interest for a few decades.[1] The experimental studies of the nonlinear spin dynamics in magnetic chains with planar anisotropy were stimulated by several theoretical considerations. For example, using the continuum limit, the equation of motion of a *classical* planar Heisenberg chain in a transverse magnetic field may be mapped to the sine-Gordon equation which is known to possess linear solutions (spin waves) and nonlinear solutions (solitons). The sine-Gordon equation has been widely used for the analysis of inelastic neutron scattering,[2] specific heat,[3] and nuclear magnetic resonance[4] studies of compounds which proved to be good realizations of the theoretical model systems. However, the quantitative agreement between the data and the corresponding theoretical predictions was often unsatisfactory due to the approximations necessary for making the mapping to the sine-Gordon model, namely uncertainties were generated by neglecting out-of-plane and *quantum* fluctuations and by employing the continuum approximation. Recently the dynamical properties of antiferromagnetic chains of *classical* spins with on-site easy-axis anisotropy, taking into account both nonlinear effects and the discreteness of the media, have received renewed attention.[5] In contrast, for over ten years, Papanicolaou and co-workers[6–9] have investigated *quantum* spin chains with strong planar anisotropy.

The energy spectrum of quantum spin chains in a strong magnetic field perpendicular to the easy plane has been studied by Papanicolaou and Psaltakis.[6] Apart from the common exchanged-coupled bound magnons, they predicted the presence of single-ion bound states. Initially, the properties of single-ion bound states were calculated for the case of easy-axis ferromagnets.[10] According to the detailed theoretical study[9] of the electron spin resonance (ESR) response of $S=1$ chains possessing a large-D phase (which is characterized by supercritical planar anisotropy of $D/J>1$, where D and J represent the single-ion anisotropy and exchange coupling, respectively), the existence of these novel quantum states should enable the observation of a transition between the one-magnon states and the single-ion bound states.

In this paper, we report interesting experimental results and a complete analysis of preliminary data[11] of the material $Ni(C_2H_8N_2)_2Ni(CN)_4$, commonly known as NENC.[12,14] The data are from a study of the temperature dependence of the intensities of selected ESR resonance lines and of the magnetic susceptibility of single crystals. Earlier experimental studies of the thermodynamic properties of NENC (Ref. 14) revealed that the compound can be considered as an $S=1$ antiferromagnetic Heisenberg chain in a large-D phase with planar anisotropy $D/k_B=6$ K and $D/J=7.5$. For large-D systems in zero magnetic field the concept of excitons and antiexcitons [hereafter abbreviated as (anti)excitons] as out of easy-plane fluctuations from the singlet ground state was proposed in a strong-coupling theory.[7] The specific heat calculated in the dilute exciton approximation is in good agreement with the low-temperature data of NENC.[14] This result stimulated further extension of the theoretical model by involving the interactions between (anti)excitons and the effect of in-plane anisotropy induced by orthorhombic therm $E[(S^x)^2-(S^y)^2]$.[8] The subsequent analysis of the experimental data reinforced the identification of NENC as an $S=1$ Heisenberg chain system with strong planar and weak in-plane anisotropy.[15] In the present work we show that ESR data of NENC can be successfully analyzed in the framework of the theoretical model.[9] The results strongly support the existence of single-ion bound states in NENC.

II. SPIN DYNAMICS OF LARGE-D SYSTEMS IN MAGNETIC FIELD

A. Exciton regime

In a magnetic field applied parallel to the hard axis, an $S=1$ Heisenberg antiferromagnetic chain may be described by the Hamiltonian[9]

$$\mathcal{H}=J\sum_i \vec{S}_i\cdot\vec{S}_{i+1}+D\sum_i (S_i^z)^2+g\mu_B B\sum_i S_i^z \qquad (1)$$

in which $D/J>1$. For magnetic fields sufficiently low with respect to D, the ground state of the Hamiltonian (1) is a disordered singlet characterized by an exponential decay of the correlation function and a finite excitation gap appears above the ground-state energy. The first excited state is an $\Sigma_i S_i^z=1$ doublet corresponding to excitons (ε) and antiexcitons ($\bar{\varepsilon}$). Higher excited states involving $\varepsilon\varepsilon$, $\varepsilon\bar{\varepsilon}$, and $\bar{\varepsilon}\bar{\varepsilon}$ pairs form either unbound states falling into the two-exciton continuum or bound states whose dispersion branches appear at the boundary of the Brillouin zone. The excitation spectrum of Hamiltonian (1) for $D/J=7.5$ in zero magnetic field is illustrated in Fig. 1. For low magnetic fields, i.e., $g\mu_B B<g\mu_B B_{c1}\approx D-2J$, the ground state remains a singlet.[9] Thus the ESR spectrum will be dominated by $k=0$ transitions from the ground state to the (anti)excitonic state at the resonance frequencies $\hbar\omega_A\approx D+2J+g\mu_B B$ and $\hbar\omega_B\approx D+2J-g\mu_B B$. The higher-order transitions (e.g., $\varepsilon\rightarrow\varepsilon\varepsilon$, $\varepsilon\rightarrow\varepsilon\bar{\varepsilon}$, ...) are responsible for the observed finite linewidth and possibly a mild temperature-dependent frequency shift of the maximum of the intensity. For $g\mu_B B_{c1}\approx D-2J$, the crossover between the antiexcitonic dispersion branch and the energy of the ground state occurs at the Brillouin-zone boundary.[9] At this crossover, the ground state ceases to be a singlet, and the model of (anti)excitons is no longer valid.

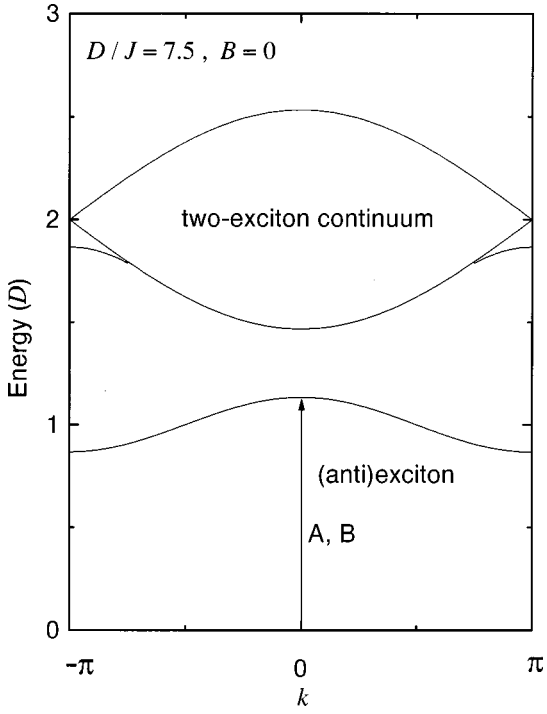

FIG. 1. The energy-level scheme (in units of D) for a $S=1$ antiferromagnetic chain with planar anisotropy and subcritical exchange interaction $D/J=7.5$ in zero magnetic field. A and B denote the $k=0$ transitions from the singlet ground state to the excitonic and antiexcitonic states, respectively.

B. Magnon regime

In sufficiently strong magnetic fields, i.e., $g\mu_B B>g\mu_B B_{c2}=D+4J$, the spins are flipped into the direction of the field, and the ferromagnetic ground state is obtained. In this regime, magnons become the elementary excitations. In the $D/J\rightarrow\infty$ limit, a one-magnon state is obtained by decreasing the azimuthal spin value by one unit at a given site. Two-magnon states can be constructed either by reducing the azimuthal spin by two units at a single site (I) or by reducing its value by one unit at two different sites (II). If the exchange interaction is taken into account, apart from the two-magnon continuum, two kinds of bound states will appear. States of type (I) are single-ion bound states. These states are characterized by a very weak dispersion even for intermediate values of D/J, and their dispersion branch is located above the two-magnon continuum. States of type (II) denote common exchange-coupled bound states emerging from the continuum at the zone boundary. The corresponding energy diagram for magnetic field parallel to the hard axis, when $g\mu_B B=3D$ and $D/J=7.5$, is illustrated in Fig. 2.

Above B_{c2}, the ground state orders ferromagnetically, as mentioned previously. Consequently at zero temperature and at $k=0$, $\delta m=1$ transitions between the ferromagnetic ground state and the one-magnon states result in the resonance frequency $\hbar\omega_c=g\mu_B B-D$ (line C in Fig. 2).[9] Processes with $\delta m=1$ at finite temperature involve the transitions between one-magnon and two-magnon states. A closer look at Fig. 2 suggests that the signal from both transitions

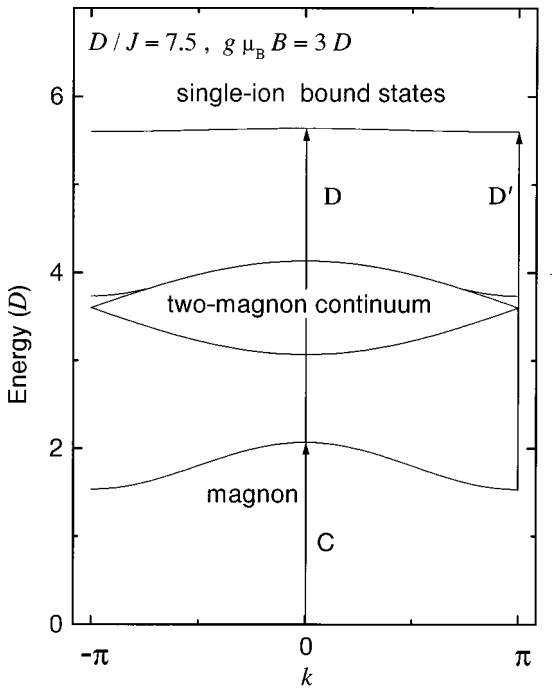

FIG. 2. The energy-level scheme (in units of D) for a $S=1$ antiferromagnetic chain with planar anisotropy, $D/J=7.5$, and in a magnetic field above the spin-flop regime ($g\mu_B B=3D$). Line C denotes the $k=0$ resonance transition between the magnetic ground state and the one-magnon state, while D and D′ denote the $k=0$ and $k=\pi$ transitions from the one-magnon to the single-ion bound states, respectively.

(i.e., from the one-magnon state into the exchange-coupled bound state and into states in the continuum) will be roughly superimposed on the C line, thereby contributing to its broadening. On the other hand, the transition from the one-magnon to the single-ion bound state is clearly distinguishable from the C line. Since this transition can occur anywhere in the Brillouin zone where a resonance condition is fulfilled, a resonance band (D, D' lines in Fig. 2) will appear instead of a sharp resonance. The width of the DD' band at low temperatures was calculated to the third order of perturbation theory, yielding[9]

$$\hbar(\omega_D-\omega_{D'})=4J-\frac{2J^2}{D}-\frac{J^3}{D^2}, \tag{2}$$

where $\hbar\omega_D=D+g\mu_B B$ and $\hbar\omega_{D'}=D+g\mu_B B-4J+(2J^2/D)+(J^3/D^2)$ are the resonance frequencies of the transitions between the one-magnon state and the single-ion bound state at $k=\pi$ and $k=0$, respectively. Finally, when combined with the values of D and J that are derived from the analysis of the thermodynamic quantities, the theoretically calculated frequency vs field diagram may be compared with the experimental results.

III. EXPERIMENTAL DETAILS

A. Crystal structure of NENC

The material NENC crystallizes in the monoclinic space group $P21/n$, $a=7.104(3)$ Å, $b=10.671(3)$ Å, $c=9.940(2)$ Å, $\beta=114.68(2)°$, $Z=2$ as revealed by structural studies performed at room temperature.[12] The structure is built up of neutral chains running along the c axis. The repeating unit is $-[Ni(C_2H_8N_2)_2-NC-Ni(CN)_2-CN]-$, and two distinct nickel(II) sites are present. In the $[Ni(CN)_4]^{2-}$ anion, the nickel is in a square planar configuration being bonded to four cyano groups through C atoms. This nickel(II) ion is diamagnetic. In the $[Ni(C_2H_8N_2)_2]^{2+}$ cation, the nickel(II) is in a distorted octahedral configuration, where four N atoms from two $C_2H_8N_2$ molecules are in the basal plane and two N atoms from the cyano groups are in apical positions. This nickel(II) ion is paramagnetic. The chain is therefore made of $S=1$ octahedral nickel(II) ions linked by diamagnetic square planar $NC-Ni(CN)_2-CN$ units. The chains are well insulated with no bonding between them. It should be mentioned that the local anisotropy axes in adjacent chains are slightly tilted with respect to the c axis.[12] Consequently, it is impossible to orient an external magnetic field parallel to the local anisotropy axes of all the sites.

B. Electron spin resonance

For experimental studies of the frequency vs field diagram, the magnetic field was applied approximately parallel to one of the local anisotropy axes (z axis). The ESR spectrometer was described elsewhere.[13] On the other hand, the temperature dependence of the intensity was studied in magnetic fields parallel to the chain axis c to ensure an equal contribution from both kinds of chains. This experiment was performed on a transmission type spectrometer capable of mm- and submm-wavelength ranges in magnetic fields up to 16 T and at the temperatures 1.6−30 K. The single crystal was nominally $1.2\times0.5\times0.3$ mm^3, and the Voigt geometry was employed. In order to detect the real shape and absolute value of the absorption with a minimum of the experimental error, amplitude modulation was used.

C. Susceptibility

Magnetic susceptibility measurements of NENC single crystals were performed in a commercial superconducting quantum interference device magnetometer using crystals weighing approximately 455 μg. The crystals were glued to weighing paper using GE 7031 varnish and placed in a gelcap which was held in a straw. The contribution of the background, which was measured independently, did not exceed 20% of the total signal and has been subtracted from the experimental data. In the experimental runs, the magnetic field of 100 mT was oriented parallel to the b and c axes.

IV. RESULTS AND DISCUSSION

Figure 3 shows the resonance frequencies vs magnetic field obtained at 4.2 K in the nominal frequency range 200–400 GHz for B approximately parallel to z and the corresponding theoretical predictions[9] for $D/k_B=6$ K, $D/J=7.5$, and $g=2.29$. It should be mentioned that for $B\|c$ the double-resonance structure observed above 12 T disappeared and only one resonance line remained. This effect has been indicated before by studying the angular dependence of the resonances.[11] Even though the NENC resonance spectrum possesses more complicated structure than predicted,[9] the ex-

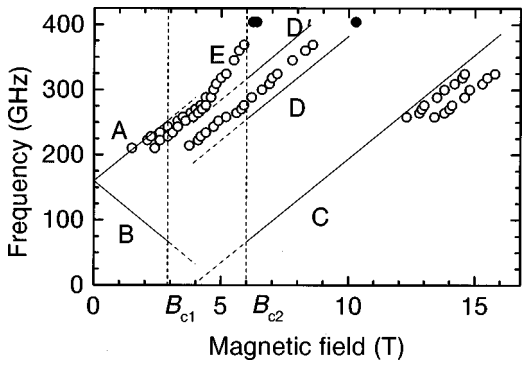

FIG. 3. The comparison between the experimental and theoretical results. The ESR data (open circles) were obtained at 4.2 K, with B approximately parallel to z. The theoretical predictions for the exciton and magnon regimes (full lines A, B, C, D, and D′) were calculated using $D/k_B=6$ K, $D/J=7.5$, as derived from the analysis of the thermodynamic results (Ref. 14) and $g=2.29$. Full circles correspond to resonances at 404 GHz, 4.2 K for $B\|c$.

perimental data reflect the main features of the model remarkably well. The extrapolation of the frequency-field dependences of the resonance lines observed below 4 T suggests the existence of two different excitation frequencies in zero magnetic field. This fact, together with the angular dependence of the resonance lines above 12 T, may indicate the presence of two slightly different positions of the Ni^{2+} ions in the octahedral surroundings in NENC.

The most important features of the experimental results shown in Fig. 3 is the appearance of the anomalous resonance line located in the DD′ band (henceforth referred to as DD′ line) and the E line. The resonances at 404 GHz (full circles) were obtained for $B\|c$, whereas the other frequencies (open circles) were taken with B approximately parallel to z. This results show that in NENC tilted local anisotropy axes do not significantly influence the resonance positions.

The temperature and the field dependence of the 404 GHz resonances for $B\|c$ are shown in Fig. 4. The intensity of the E line decreases with increasing temperature indicating ground-state excitations. According to Fig. 2 it can only be a $k=0$ ground-state excitation to the single-ion bound state. Such a transition is forbidden in a model assuming only planar anisotropy and exchange coupling. However, the transitions may arise from the combined effect of in-plane anisotropy and exchange coupling.[9] Below 7 K, the double peak structure of the E line may be ascribed to the two different

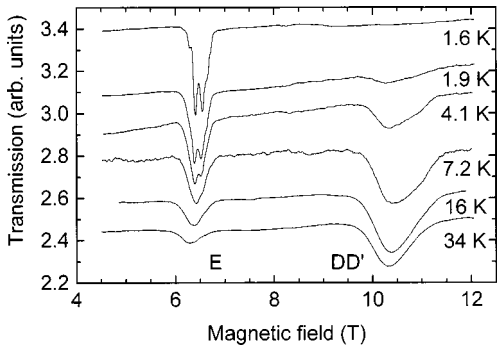

FIG. 4. The comparison of the shapes of E and DD′ resonance lines studied at 404 GHz for $B\|c$.

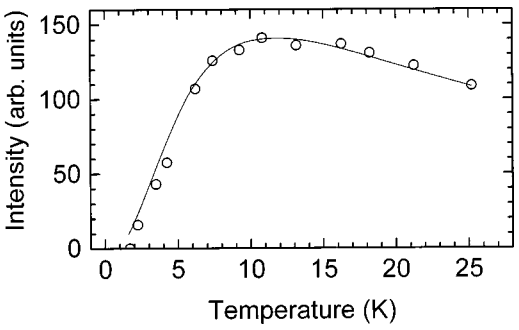

FIG. 5. Temperature dependence of the integrated intensity of the anomalous (DD′) line studied at 404 GHz, maximum of the absorption intensity corresponding to 10.3 T, with $B\|c$. The full line represents the simplified theoretical fit as discussed in the text.

surroundings of the Ni^{2+} ions as discussed above.

The DD′ line also shown in Fig. 4 has a different temperature dependence of the intensity. Below 10 K the intensity decreases with the decreasing temperature (see also Fig. 5). This behavior indicates a transition between excited states. The position and slope of this DD′ line suggest that it can be ascribed to the transitions between one-magnon states and single-ion bound states as follows from Figs. 2 and 3. The comparison of the half-widths of the E and DD′ lines provides insight into the different nature of both transitions (Fig. 4). Unlike the E line for which transitions from the ground state at $k=0$ are proposed, a transition at any finite k value, for which the resonance condition is fulfilled while sweeping the magnetic field, will contribute to the DD′ line. Thus the half-width of the DD′ line should be significantly larger than that of E line. As seen from Fig. 5, the half-width of the DD′ line is approximately 1 T ($\approx$30 GHz). On the other hand, the theoretically calculated value of the width of the DD′ band is about 2 T, when using $D/k_B=6$ K and $D/J=7.5$. This discrepancy could be ascribed to the presence of in-plane anisotropy indicated by the observation of the E line.[9] The subtle effects associated with the presence of in-plane anisotropy were demonstrated during the reanalysis of the thermodynamic quantities,[15] where the incorporation of a finite E term in the calculation significantly reduced the value of J while leaving D practically unchanged. As can be seen from Eq. (2), decreasing the J value causes the narrowing the DD' band.

The temperature dependence of the integrated intensity of the DD′ line is shown in more detail in Fig. 5. This dependence could be theoretically calculated using both density of states for the magnon branch (see Fig. 6 in Ref. 9) and the transition probabilities. Since the latter quantities are not known a simplified fit was made considering only the $k=0$ and $k=\pi$ transitions (indicated by D and D′ in Fig. 2) because for these k values the substantial contribution to the integrated intensity can be expected due to the enhanced density of states. The magnitudes of the gaps of one-magnon states at $k=0$ and $k=\pi$ were calculated using the aforementioned D, J, and g values, and 404-GHz radiation frequency. The calculation yielded 217 and 92 GHz for $k=0$ and $k=\pi$, respectively. Using the Boltzmann statistics and the obtained values of the gaps the experimental data of the integrated intensity were fitted, the relative intensity contributions of the transitions at $k=0$ and $k=\pi$ were taken as the

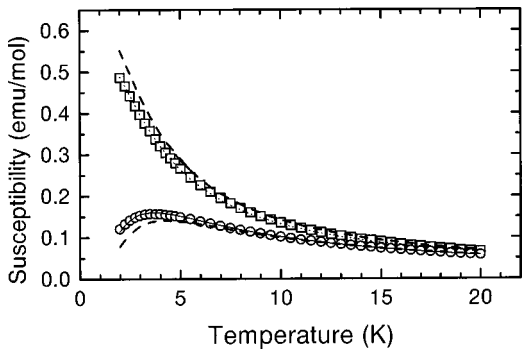

FIG. 6. Temperature dependence of the susceptibility of NENC measured in a magnetic field parallel to the *c* axis (circles) and the *b* axis (squares). Dashed lines represent the theoretical predictions for both directions using $g=2.29$, $D/k_B=6.3$ K, $E/k_B=0.9$ K, and $J/k_B=0.15$ K, as obtained from the analysis from powder susceptibility data (Ref. 15). The results of the independent fits of both data sets are denoted by the solid and dotted lines. See the text for a more detailed discussion and the values of the parameters.

fitting parameters. As can be seen in Fig. 5 for the ratio 3:1 a good agreement with the experimental data was obtained. It should be noted that the contribution from the enhanced density of states at $k=0$ and $k=\pi$ could also be discerned from the irregular shape of DD′ in Fig. 4.

In addition, the presence of the in-plane anisotropy, as well as the effect of the tilted local anisotropy axes, may also be detected in magnetic susceptibility studies using single crystals. At present for large-D systems, the susceptibility is the only quantity in which a finite magnetic field has been incorporated into a theoretical description along with finite values of J, D, and E. In the experiment, the magnetic field was oriented parallel to the *c* and *b* axes, while the theoretical predictions incorporating D, J, and E are available for fields parallel and perpendicular to the hard axis. The comparison between the experimental data and the theoretical predictions, using the values of parameters obtained from the analysis of powder susceptibility, is illustrated in Fig. 6. Clearly, the experimental susceptibility data parallel to *c* axis lie above the theoretical prediction, while the opposite situation exists for the susceptibility parallel to *b* axis. This effect can be ascribed to the tilting of the local anisotropy axis from the direction of the magnetic field. It should be stressed that the agreement cannot be improved by a physically meaningful modification of the values of the parameters. For example, suitable fits for each direction can be obtained only after significant renormalization of the parameters for each direction, namely $g_{\|}=2.25$, $D/k_B=5.5$ K, $E/k_B=1.5$ K, $J/k_B=0.01$ K for $B\|c$ and $g_{\perp}=2.23$, $D/k_B=6.5$ K, $E/k_B=0.15$ K, $J/k_B=0.12$ K for $B\|b$.

V. CONCLUSION

In summary, the position, slope, and temperature dependence of the anomalous (DD′) resonance line and the presence of the E line strongly suggests that these are the transitions between the one-magnon and the single-ion bound states and the ground-state excitation to single-ion bound states, respectively. However, as was demonstrated by the observation of the additional E line as well as by the susceptibility studies, finite in-plane anisotropy and the tilted local anisotropy axes do not allow for more detailed studies in NENC. More specifically, we assume that the aforementioned structural features of the material prevent the observation of the theoretically predicted double peak structure in the anomalous resonance DD′ line. Consequently, the possibility of synthesizing another compound of the $Ni(X)_2Ni(CN)_4$ class, i.e., a system with a tilt-free orientation of the local anisotropy axes and a weaker in-plane anisotropy, is under investigation.[16] In addition, the detailed quantitative description of all the observed resonance lines requires the incorporation of in-plane anisotropy into the theoretical model.[9] Since, according to our knowledge, magnetic excitations in $S=1$ planar Heisenberg chains in the spin-flop regime ($B_{c1}<B<B_{c2}$) have not been theoretically studied yet, the presented results might stimulate a theoretical investigation of the excitation spectrum of these systems in the aforementioned field range. Finally, it would be interesting to conduct analogous experimental studies using $S=1$ planar Heisenberg ferromagnets and $S=1$ Heisenberg chains with easy-axis anisotropy, since single-ion bound states have also been predicted in these systems.[9,6]

ACKNOWLEDGMENTS

We are grateful to N. Papanicolaou for a number of enlightening discussions and careful reading of the manuscript. We are indebted to J. Černák for the synthesis of the single crystals. This work was supported, in part, by Deutsche Forschungsgemeinschaft (DFG) through Grant No. SFB252 and by the National Science Foundation (Grant No. INT-9722935). Two of us (A.O. and M.O.) appreciate the support from the Greek-Slovak bilateral program, while S.Z. is grateful for the support from the Alexander von Humboldt Foundation.

[1] M. Mikeska and M. Steiner, Adv. Phys. **40**, 191 (1991), and references therein.
[2] S. E. Nagler, W. J. L. Buyers, R. L. Armstrong, and B. Briat, J. Appl. Phys. **55**, 1856 (1984).
[3] A. M. C. Tinus, W. J. M. de Jonge, and K. Kopinga, Phys. Rev. B **32**, 3154 (1985).
[4] K. Kopinga, A. M. C. Tinus, W. J. M. de Jonge, and G. C. de Vries, Phys. Rev. B **36**, 5398 (1987).
[5] R. Lai and A. J. Sievers, Phys. Rev. B **57**, 3433 (1998), and references therein.
[6] N. Papanicolaou and G. C. Psaltakis, Phys. Rev. B **35**, 342 (1987).
[7] N. Papanicolaou and P. Spathis, J. Phys.: Condens. Matter **2**, 6575 (1990).
[8] N. Papanicolaou and N. Spathis, Phys. Rev. B **52**, 16 001 (1995).
[9] N. Papanicolaou, A. Orendáčová, and M. Orendáč, Phys. Rev. B **56**, 8786 (1997).
[10] R. Silberglitt and J. B. Torrance, Phys. Rev. B **2**, 772 (1970).
[11] S. A. Zvyagin, T. Rieth, M. Sieling, S. Schmidt, and B. Lüthi, Czech. J. Phys. **46**, 1937 (1996).

[12] J. Černák, J. Chomič, D. Baloghová, and M. D. Jurčo, Acta Crystallogr., Sect. C: Cryst. Struct. Commun. **C44**, 1902 (1988).
[13] V. V. Eremenko, S. A. Zvyagin, and V. V. Pishko, Fiz. Nizk. Temp. **18**, 255 (1992) [Sov. J. Low Temp. Phys. **18**, 175 (1992)].
[14] M. Orendáč, A. Orendáčová, J. Černák, A. Feher, P. J. C. Signore, M. W. Meisel, S. Merah, and M. Verdaguer, Phys. Rev. B **52**, 3435 (1995).
[15] A. Orendáčová, M. Orendáč, A. Feher, M. W. Meisel, P. J. C. Signore, S. Merah, and M. Verdaguer, Czech. J. Phys. **46**, 1939 (1996).
[16] J. Černák (private communication).